Indian Journal of Chemistry
Vol. 58A, May 2019, pp. 554-560

pH Dependant competitive *N*-de-ethylation and degradation of Rhodamine B photocatalyzed by cationic surfactant stabilized ZnS nanoparticles

Wandibahun Warjri & Devendra P S Negi*
Department of Chemistry, North-Eastern Hill University, Shillong 793 022, India
Email: dpsnegi@nehu.ac.in/ devnegi@yahoo.com

Received 20 September 2018; revised and accepted 4 April 2019

The role of solution pH on the photodegradation behaviour of Rhodamine B (RhB), an industrially important dye has been examined. ZnS nanoparticles (NPs) have been synthesized using cetyltrimethylammonium bromide (CTAB) as a stabilizing agent and characterized by UV-visible spectroscopy, powder X-ray diffraction (PXRD) and transmission electron microscopy (TEM). The photocatalytic activity of the semiconductor has been evaluated by studying the degradation of RhB at various solution pH using 254 nm ultra violet (UV) light. At pH 4, the absorption peak of RhB has been blue shifted by 57 nm within 30 min, suggesting a 4-fold *N*-de-ethylation. However, at pH 11, the blue shift in the absorption band has been only about 20 nm during 30 min of irradiation. Besides, the band has been found to diminish with increase in irradiation time indicating the degradation of the dye. The mechanistic investigations suggested that the hydroxyl radicals generated in the solution were responsible for both the de-ethylation and degradation of RhB in the presence of the ZnS NPs. The potential application of such a study lies in the optimization of the reaction parameters for the treatment of waste water containing such dyes.

Keywords: Photocatalytic, Semiconductors, Degradation, Irradiation, Rhodamine B

Semiconductor photocatalysts have been in the scientific focus for their ability to convert solar energy into chemical energy. The progress of semiconductor-based nanocomposites as photocatalysts has been reviewed recently. Various solar energy conversion related reactions such as water splitting, carbon dioxide reduction, nitrogen fixation and photosynthesis have been discussed in literature[1]. ZnS is a wide band gap semiconductor and absorbs in the ultra violet region of the electromagnetic spectrum. It is a good photocatalyst because of fast generation of electron-hole pairs by photoexcitation and the negative reduction potential of conduction band electrons[2]. It does not have toxicity related issues as associated with cadmium based semiconductors such as CdS, CdSe and CdTe. For photocatalytic applications, colloidal semiconductors have several advantages over particulate semiconductors. Firstly, there is no need for separation of the photocatalyst and the probe molecule for monitoring the reaction using UV-visible spectrophotometry. Secondly, the stabilizer molecule employed during the nano-sized semiconductor synthesis could facilitate the adsorption of the substrate on the surface of the photocatalyst. Surfactants are surface active agents and are characterized by a polar head group and a hydrophobic tail. There are some literature reports on the synthesis of semiconductor nanoparticles using both cationic[3,4] and anionic[5-7] surfactants as stabilizer molecules.

Coloured waste water released from textile industries is hazardous for aquatic life since it contains harmful organic dyes[8]. Adequate treatment of such pollutants is necessary before release of the waste water into natural water bodies such as rivers and lakes. Rhodamine B (RhB) is an *N*-alkylamine containing dye, which is known to degrade through two competitive pathways: an *N*-dealkylation process and a cleavage of the chromophore structure[9-15]. The products of the de-ethylation have also been separated and characterized by earlier workers[12].

In the present work, we have studied the photocatalytic degradation of RhB using cetyltriammonium bromide (CTAB) stabilized ZnS nanoparticles (NPs). The competition between the two pathways has been analysed as a function of the solution pH.

Materials and Methods

Chemicals

Zinc nitrate hexahydrate (98%) and hydrochoric acid (35%) were purchased from Merck.

cetyltrimethylammonium bromide (99%), rhodamine B (98%), sodium hydroxide (98%) and terephthalic acid (98%) were obtained from Himedia. Sodium sulphide (98%) was purchased from Acros. All other chemicals were of analytical grade. The water used for preparing the solutions was purified through distillation.

Instrumentation and characterisation

The optical absorption spectra of the ZnS NPs were recorded on a PerkinElmer Lambda 25 UV-visible spectrophotometer. TEM measurements were performed on a JEM-2100 instrument operating at 200 kV. The crystal structure of the colloidal ZnS NPs was characterised via powder X-ray diffraction (PXRD) using GNR Analytical Instruments Group Explorer. The samples were prepared by ultracentrifugation of the colloidal semiconductor. The particles were washed with water and ethanol several times and then dried at 120 °C. Photoluminescence spectra were recorded using Hitachi 4500 spectofluorimeter. The photocatalytic activity measurements were carried out using an immersion type photoreactor (Model : HP-SLJV16254) obtained from Heber Scientific, Chennai, India. The photoreactor was equipped with a 16 W low pressure mercury vapour lamp emitting 254 nm light. A 30 W tungsten visible lamp was used for visible light irradiation.

Photocatalytic activity measurements

The photocatalytic activity of the as-synthesized ZnS NPs was evaluated by the degradation of RhB in aqueous solution under ultraviolet irradiation. The photocatalytic experiments were carried out in a 250 mL borosilicate reaction vessel immersed within a quartz tube holding the 16 W mercury lamp emitting at 254 nm. The reaction vessel has an outer jacketed wall to recirculate the coolant to remove the heat generated from the lamp. Typically, the reaction mixture was prepared as follows: 100 mL of the dye (2×10^{-5} M) was added to 100 mL of colloidal ZnS NPs and the solution was adjusted to the desired pH value (4-11) with NaOH and HCl. Prior to irradiation, the solution was stirred magnetically in the dark for 1 h to establish an adsorption-desorption equilibrium between the NPs and the dye. The solution was stirred before and during the illumination. Aliquots of the sample (3 mL) solution were taken out at certain interval time (10 min) to monitor the progress of the reaction using PerkinElmer Lambda 25 UV-visible spectrophotometer.

Synthesis of the ZnS NPs

The colloidal ZnS NPs were prepared using the method reported by Mehta *et al.*,[3] with some modifications (order of addition of the precursors). Zinc nitrate hexahydrate ($Zn(NO_3)_2.6H_2O$) as a Zn^{2+} ion source and sodium sulphide (Na_2S) as a S^{2-} ion source were used as precursors for the synthesis of the ZnS NPs. CTAB ($C_{19}H_{42}NBr$) was used as a stabilising agent. All the reagents used were of analytical grade and used without further purification. Molar concentrations of the precursors and stabilizer was prepared in distilled water. The synthesis was carried out at room temperature (20 °C). In a 500 mL flask, 0.5 mL of 0.4 M $Zn(NO_3)_2.6H_2O$ was added to 394 mL distilled water. This was followed by the addition of 5 ml of 0.4 M CTAB to obtain a micellar concentration of 5 mM. Then 0.5 mL of 0.4 M Na_2S was injected into the solution under vigorous stirring. The molar ratio obtained for Zn^{2+}/S^{2-} was 1:1. A transparent solution of ZnS NPs was obtained.

Results and Discussion

Characterization of the CTAB stabilized ZnS NPs

The UV-visible spectrum of the ZnS NPs has been displayed in Supplementary Data, Fig. S1. The spectrum lies in the ultra violet region and does not contain any absorption band. The optical band gap of the semiconductor was calculated from the Tauc plot (Fig. S2). The band gap is obtained by the point of intersection of the tangent to the curve with the *x* axis. The band gap of ZnS was found to be 3.75 eV. The crystalline nature of the material was verified by recording the PXRD pattern (Fig. 1). The peaks observed at 28.6, 48 and 56.8 correspond to the (111), (220) and (311) planes of cubic ZnS[3]. The particle size of the semiconductor was determined by TEM

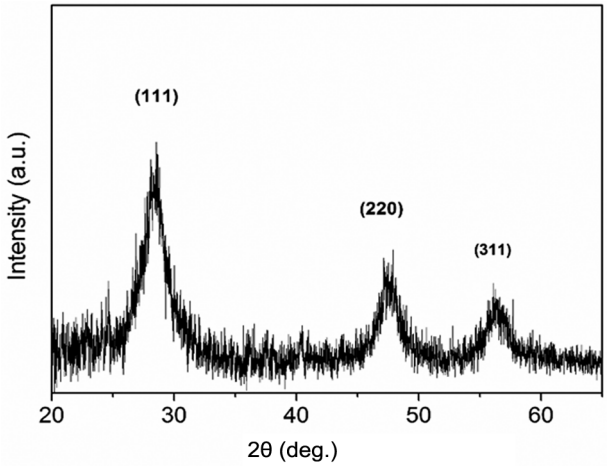

Fig. 1 — PXRD pattern of the ZnS NPs.

analysis. The TEM image of the ZnS particles has been shown in Fig. 2. The particles appearing in this image have been agglomerated during the drying process. The particles were 5–7 nm in size. The high resolution TEM image (Fig. 3) was recorded in order to verify the shape and crystallinity of an individual particle. The crystalline planes of ZnS can be clearly seen in this image. The *d*-spacing value was calculated to be 0.31 nm. The selected area electron diffraction pattern of the particles is shown as an inset in Fig. 3. The concentric rings seen in the image reveal the crystalline nature of the material.

Photocatalytic transformation of RhB using CTAB stabilized ZnS NPs

The reaction mixture containing ZnS NPs and RhB (1×10^{-5} M) was irradiated using 254 nm light. The UV-visible spectra of the reaction mixture at pH 4.0 have been displayed in Fig. 4. The 554 nm absorption band of RhB was found to diminish and simultaneously undergo blue-shift upon increase in the irradiation time. The colour of the dye was found to change from pink to light green. Earlier researchers have also reported a blue-shift in the absorption peak while studying the degradation of RhB using other semiconductor particles[9-13,16]. The observed spectral changes can be attributed to the stepwise de-ethylation of RhB. Each de-ethylation step leads to a hypsochromic shift of ~15 nm and a 60 nm shift could be attributed to the formation of a 4-fold de-ethylated RhB[10]. The absorption peak of RhB was found to be shifted to 497 nm after 60 min of irradiation. Therefore, the λ_{max} of RhB was blue shifted by 57 nm. It suggested that a 4-fold de-ethylation of RhB occurred during the irradiation, if the 3 nm difference from the expected value is ignored.

To test whether the de-ethylation of RhB was indeed catalyzed by the ZnS NPs, a control experiment was carried out where RhB was irradiated using 254 nm light in the absence of the photocatalyst. The UV-visible spectra of the dye at different irradiation times have been displayed (Supplementary Data, Fig. S3). It is seen from this figure that there was no change in the λ_{max} of the dye upon increase in the irradiation time. However, the absorption due to the dye was found to be reduced to a small extent. These spectral changes indicate that there was no de-ethylation of the dye in the absence of the semiconductor.

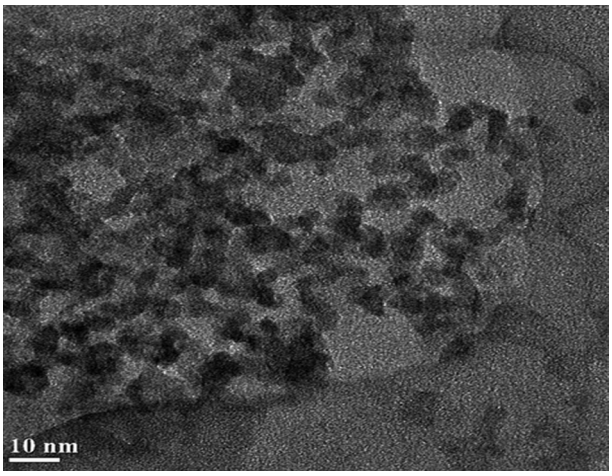

Fig. 2 — TEM image of the ZnS NPs.

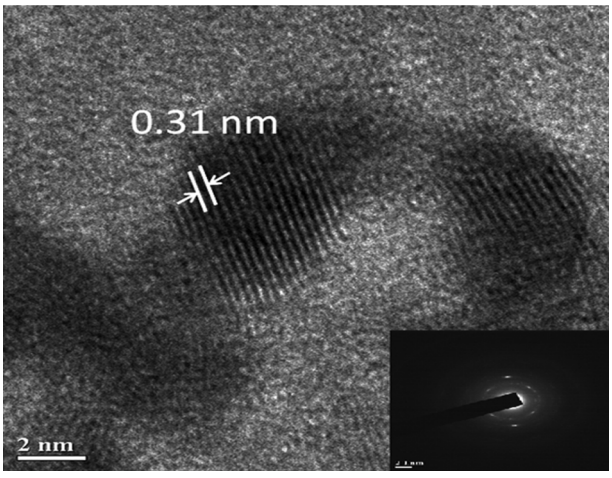

Fig. 3 — High resolution TEM image and SAED pattern (inset) of the ZnS NPs.

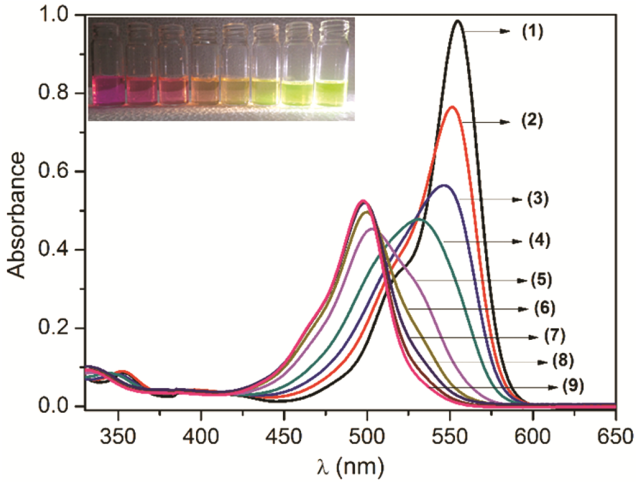

Fig. 4 — UV-Visible spectra of the reaction mixture containing ZnS NPs and RhB (1×10^{-5} M) at pH 4 as a function of the irradiation time(in min): 0, 2.5, 5, 10, 20, 30, 40, 50, 60 (curves 1-9 respectively).

It has been reported earlier that the semiconductor catalyzed de-ethylation of RhB was primarily a surface process[11,16]. The RhB molecule upon excitation transfers an electron to the conduction band of the semiconductor. The radical cation of the dye thus produced upon subsequent reactions results in the formation of the de-ethylated product[11]. To test this possibility, we carried out the irradiation of the reaction mixture containing the dye and the ZnS NPs in the presence of visible light. Since ZnS is transparent to visible radiation, it will not undergo excitation to produce electron-hole pairs. The UV-visible spectra of the reaction mixture containing RhB (1×10^{-5} M) and the ZnS NPs has been displayed (Supplementary Data, Fig. S4). It is seen that there was no blue-shift in the absorption peak of the dye with increase in irradiation time. However, there was a slight decrease in the absorbance of the dye with the time of irradiation, suggesting degradation of the dye. It suggests that the photoexcited dye cannot transfer an electron to the conduction band of ZnS. This is understandable since the conduction band edge of ZnS is more negative than that of the other semiconductors[17].

Based on the above results the de-ethylation of RhB photocatalyzed by the ZnS NPs could occur as follows. Photoexcitation of the ZnS NPs by 254 nm light results in the excitation of an electron from the valence band (V.B.) to the conduction band (C.B.) as shown in the eqn 1. The vacancy left in the V.B. is designated as a hole (h^+). The hole extracts an electron from the adsorbed dye thus producing the radical cation (eqn 2). The radical cation of the dye upon further reaction could produce the de-ethylated products (eqn 3).

$$ZnS + h\nu \rightarrow e\,(C.B.) + h\,(V.B.) \quad \ldots (1)$$

$$RhB + h^+(V.B.) \rightarrow RhB^{\bullet+} \quad \ldots (2)$$

$$RhB^{\bullet+} \rightarrow de-ethylated\ products \quad \ldots (3)$$

Liquid Chromatography Mass Spectrometry (LCMS) measurements were carried out to determine the intermediates formed during the de-ethylation of RhB. The intermediates depicting λ_{max} of 541, 525, 510 and 497 nm were separated and analysed by LCMS. The mass spectra of RhB and the various intermediates have been displayed as Supplementary Data Figs S5-S9. The mass peaks at *m*/*z* 443.2, 415.2, 387.2, 359.1 and 330.7 in these figures correspond to RhB and its de-ethylated intermediates. These peaks differ approximately by 28 mass units which confirms the sequential *N*-de-ethylation of RhB. On the basis of the above results, the fragmentation mechanism of rhodamine B has been displayed in Scheme 1.

In contrast to the results obtained at pH 4.0, the reaction between RhB and the ZnS NPs at pH 11 showed a completely different behaviour. The absorption spectra of RhB in the presence of the ZnS NPs at pH 11 as a function of irradiation time have been displayed in Fig. 5. The absorption peak of RhB at 554 nm was found to decrease in intensity along with a gradual blue shift. Notably, the colour of the dye was bleached after 60 min of irradiation. It indicates that RhB primarily underwent degradation at pH 11 in contrast to the de-ethylation observed at pH 4. The degradation of RhB in the presence of the ZnS NPs was also investigated at pH values between 4 and 11. The absorption spectra of the reaction mixture containing RhB and ZnS NPs at pH 6, 8 and 10 as a function of irradiation time have been displayed (Supplementary Data, Fig. S10-S12). It is evident that the extent of de-ethylation was reduced upon increasing the pH of the solution. The plot of the blue-shift in the absorption peak of RhB at different pH with change in irradiation time has been displayed in Fig. S13. It is evident from the plot that the shift follows a similar trend for pH 6–8. However, at pH 10 it takes much longer time for the de-ethylation process to be completed. At pH 11, the de-ethylation is not complete even after 60 min of irradiation. These results suggest that at lower pH, de-ethylation is favoured whereas at higher pH, degradation of the dye is favourable.

Mechanistic aspects of the competitive de-ethylation and photodegradation of RhB in the presence of ZnS NPs

The chemical structure of the dye is displayed in the Fig. S14. The pk_a of the carboxylic acid group is reported to be 3.22[18]. Therefore, at pH 4, the carboxylic acid group will be predominantly in the deprotonated state. It was proposed by Mehta *et al.*[19] that the ZnS NPs are stabilized in the solution by the CTAB surfactants forming a micelle like structure around the ZnS particles with the cationic head group pointing outwardly (towards the bulk solution) (Fig. S15). Therefore, the RhB molecules will not experience repulsion from the positively charged head group of the CTAB surfactants surrounding the ZnS NPs. Hence, at pH 4, many of the RhB molecules can diffuse to the surface of the ZnS NPs and form a radical cation by transferring an electron to the photogenerated hole. It was reported by Wu and co-workers that hydroxyl radicals ($OH^{\bullet}$) were effective

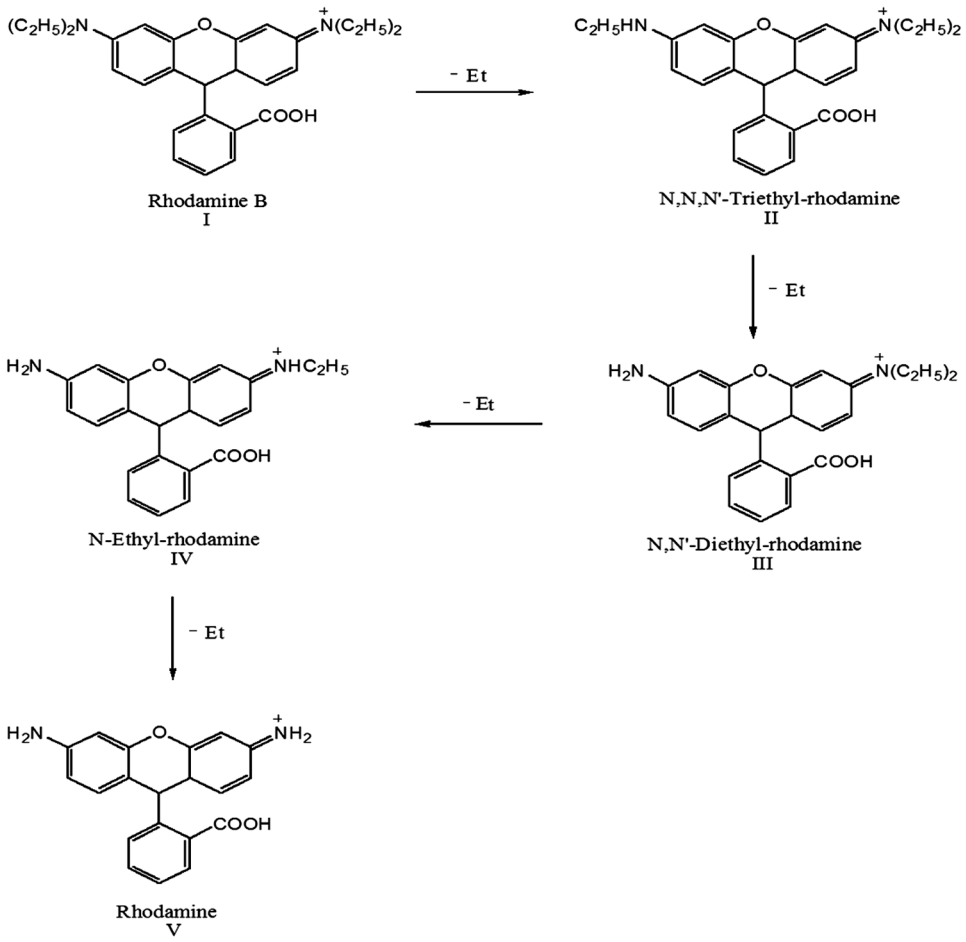

Fragmentation mechanism of RhB in the presence of ZnS NPs

Scheme 1

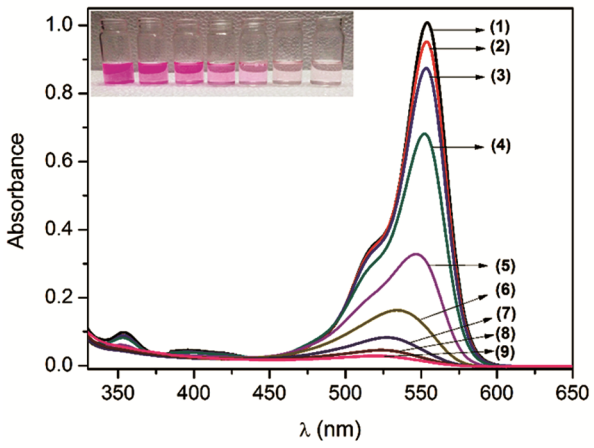

Fig. 5 — UV-Visible spectra of the reaction mixture containing ZnS NPs and RhB (1×10^{-5} M) at pH 11 as a function of irradiation time (in min): 0, 2.5, 5, 10, 20, 30, 40, 50, 60 (curves 1-9 respectively).

in causing the de-ethylation of RhB[11]. To determine whether the $OH^{\bullet}$ or the photogenerated electron was necessary for the de-ethylation of the dye in the present work, we carried out the irradiation of the reaction mixture containing RhB and the ZnS NPs in the presence of 2 mM *tert*-butyl alcohol, a known $O\dot{H}^{\bullet}$ scavenger[20] and 2 mM $FeCl_3$, an electron scavenger[13]. The plot of wavelength shift with irradiation time in the absence and presence of the scavengers has been shown in Fig. S16. The extent of de-ethylation was severely hindered in the presence of the $OH^{\bullet}$ scavenger. However, in the presence of the electron scavenger, the de-ethylation was affected but not considerably. It suggests that de-ethylation of RhB after the initial formation of the radical cation was caused by the hydroxyl radicals generated in the solution. The $OH^{\bullet}$ can be generated in acidic solution in the following manner. The oxygen molecules

adsorbed on the surface of the ZnS NPs to form super oxide radical ion, $O_2^{\bullet-}$. The superoxide radical ion upon protonation produces $HOO^{\bullet}$ radical. The latter reacts with a photogenerated electron to form H_2O_2 which further reacts with an electron to form $OH^{\bullet}$[11].

At higher pH, say at pH 10 and 11, there is a competition between the dye molecules and the OH^- ions for the photogenerated holes. The OH^- ions can diffuse much faster to the particle surface than the bulky RhB molecules. As a result, very few RhB molecules can trap the holes to form the radical cation. Hence the extent of de-ethylation decreases at pH 10 and 11. The reaction between the OH^- ions and the photogenerated hole results in the formation of hydroxyl radical[21]. The experimental evidence for the generation of $OH^{\bullet}$ at pH 11 was obtained by using terephthalic acid (TA) as a fluorescence probe. It is known that OH^- reacts with TA and generates TAOH which emits fluorescence at 426 nm on excitation at 312 nm[22]. The fluorescence spectra of the solution containing ZnS NPs in the presence of 2 mM TA at different irradiation time have been displayed in Fig. S17. It is seen from this figure that the fluorescence band at 426 nm due to TAOH was found to increase with the time of irradiation. It indicates that more and more $OH^{\bullet}$ were generated with increase in the irradiation time.

To determine whether the high concentration of $OH^{\bullet}$ was necessary for the degradation of RhB at pH 11, the irradiation of the dye was carried out in the presence of the ZnS NPs at the same pH. The plots of C_t/C_0 versus irradiation time in the absence and presence of scavengers and the ZnS NPs have been displayed in Fig. S18. It is seen from this plot that the degradation of RhB in the absence of the ZnS NPs was negligible. It indicates the crucial role of the semiconductor as a photocatalyst for the degradation of the dye. The presence of 2 mM ammonium oxalate, a hole scavenger[23], resulted in the decrease in the rate of degradation of the dye. However, the presence of 2 mM *tert*-butyl alcohol, a $OH^{\bullet}$ scavenger, resulted in much larger decrease in the degradation of RhB. These results indicate that the $OH^{\bullet}$ radicals were primarily responsible for the degradation of the dye.

Conclusions

The photocatalytic transformation of RhB in the presence of the ZnS NPs was found to be pH dependant. At pH 4, the dye underwent a 4-fold *N*-de-ethylation. However, at pH 11, photodegradation was the preferred pathway. At lower pH, the dye molecules scavenge the photogenerated hole on the semiconductor surface and form a radical cation. The radical cation upon further reaction with OH^- resulted in the de-ethylation. However, at higher pH, the $OH^{\bullet}$ ions present in the solution could scavenge the photogenerated holes since the bulky dye molecules diffuse much slower than the $OH^{\bullet}$ ions to the surface of the ZnS NPs. The $OH^{\bullet}$ thus formed, attack the chromophore of the RhB molecules present in the solution, resulting in their degradation.

Supplementary Data

Supplementary data associated with this article are available in the electronic form at http://www.niscair.res.in/jinfo/ijca/IJCA_58A(05)554-560_SupplData.pdf.

Acknowledgement

The present research work was financially supported by the University Grants Commission (award of 'Centre for Advanced Studies in Chemistry' status to our department), New Delhi. The authors thank the Sophisticated Analytical Instrument Facility (SAIF), North Eastern Hill University (NEHU), for the TEM measurements. The XRD facility of the Nanotechnology Department, NEHU, is gratefully acknowledged. The author also thank the SAIF, Central Drug Research Institute, Lucknow, for the LCMS analysis.

References

1 Wang F, Li Q & Xu D, *Adv Energy Mater,* 7 (2017) 1700529.

2 Hu J S, Ren L L, Guo Y G, Liang H P, Cao A M, Wan L J & Bai C L, *Angew Chem Int Ed,* 44 (2005) 1269.

3 Mehta S K, Kumar S, Chaudhary S, Bhasin K K & Gradzielski M, *Nanoscale Res Lett,* 4 (2009) 17.

4 Praus P, Dvorský R, Horínková P, Pospíšil M & Kovář P, *J Coll Interf Sci,* 377 (2012) 58.

5 Mitra D, Chakraborty I & Moulik S P, *Coll J,* 67 (2005) 445.

6 Dixit N & Soni H P, *Superlattice Microst,* 65 (2014) 344.

7 Devi L M & Negi D P S*, Ind J Chem,* 54A (2015) 1440.

8 Devi L M & Negi D P S, *Mater Chem Phys,* 141 (2013) 797.

9 Chen F, Zhao J & Hidaka H, *Int J Photoenergy,* 5 (2003) 209.

10 Merka O, Yarovyi V, Bahnemann D W & Wark M, *J Phys Chem C,* 115 (2011) 8014.

11 Wu T, Liu G, Zhao J, Hidaka H & Serpone N, *J Phys Chem B,* 102 (1998) 5845.

12 Yu K, Yang S, He H, Sun C, Gu C & Ju Y, *J Phys Chem A,* 113 (2009) 10024.

13 Qu P, Zhao J, Shen T & Hidaka H, *J Mol Cat A,* 129 (1998) 257.

14 Wang P, Cheng M & Zhang Z, *J Saudi Chem Soc,* 18 (2014) 308.

15 Hu X, Mohamood T, Ma W, Chen C & Zhao J, *J Phys Chem B,* 110 (2006) 26012.
16 Watanabe T, Takizawa T & Honda K, *J Phys Chem,* 81 (1977) 1845.
17 Palmisano G, Augugliaro V, Pagliaro M & Palmisano L, *Chem Comm,* (2007) 3425.
18 Moreno-Villoslada I, Jofré M, Miranda V, González R, Sotelo T, Hess S & Rivas B L, *J Phys Chem B,* 110 (2006) 11809.
19 Mehta S K, Kumar S & Gradzielski M, *J Coll Interf Sci*, 360 (2011) 497.
20 Zhang N, Liu S, Fu X & Xu Y J, *J Phys Chem C,* 115 (2011) 9136.
21 Tennakone K, Thaminimule C T K, Senadeera S & Kumarasinghe A R, *J Photochem Photobiol A,* 70 (1993) 193.
22 Hirakawa T & Nosaka Y, *Langmuir,* 18 (2002) 3247.
23 Warjri W & Negi D P S, *Mater Res Express,* 3 (2016) 095004.